1.8 Concept of Ceramics-free Coaxial Waveguide

Hiroyuki ARAI
Division of Electrical and Computer Engineering, Faculty of Engineering
Yokohama National University, Yokohama-shi, Kanagawa 240, Japan

Abstract

A critical key point of the ITER IC antenna is ceramics support of an internal conductor of a coaxial antenna feeder close to the plasma, because dielectric loss tangent of ceramics enhanced due to neutron irradiation limits significantly the antenna injection power. This paper presents a ceramics-free waveguide to overcome this problem by a T-shaped ridged waveguide with arms for the mechanical support. This ridged waveguide has a low cutoff frequency for its small cross section, which has been proposed for the conceptual design study of Fusion Experimental Reactor (FER) IC system and the high frequency supplementary IC system for ITER.

This paper presents the concept of ceramics-free coaxial waveguide consisting of the coaxial-line and the ridged waveguide. This paper also presents the cutoff frequency and the electric field distribution of the ridged waveguide calculated by a finite element method and an approximate method. The power handling capability more than 3MW is evaluated by using the transmission-line theory and the optimized antenna impedance considering the ITER plasma parameters. We verify this transmission-line model by one-tenth scale models experimentally.

1. Ceramics-free coaxial waveguide

A mechanical support of an inner conductor of a coaxial-line is quarter wavelength stub shown in Fig. 1. A reflection coefficient by this junction is calculated by the equivalent circuit shown in Fig. 1 as,

$$\Gamma = \frac{Y_o - Y_s}{Y_o + Y_s} = -\frac{1}{1 + 2j\tan(\beta l)} \quad . \tag{1}$$

where Y_s is the stub admittance , $\beta = 2\pi/\lambda$, and the stub length is l. The reflection coefficient at junction is shown in Table 1. A frequency band width is $\pm 40\%$ for power reflection less than 10%, which is not wide enough for an application of the ITER system[1]. Other disadvantages of the stub support are that its structure is not suitable for modular design and the mechanical support is not so strong. Therefore waveguide concept is required for mechanical support for coaxial-line.

Figure 2 shows ceramics-free coaxial waveguide consists of coaxial-line and ceramics-free waveguide for mechanical support. For wide frequency band operation, the junction by the ridged waveguide is used below a cutoff. The reflection below the cutoff from the ridged waveguide is calculated by the cutoff waveguide theory.

$$\Gamma = exp\{-\sqrt{k_c^2 - k^2}l\} \tag{2}$$

where k is wavenumber in free space and k_c is cutoff wavenumber of ridged waveguide. Figure 3 shows calculated reflection power S_{11} from the junction. The S_{11} is less than 10% above 10MHz for the cutoff frequency of the ridged waveguide being less than 40MHz. This frequency band width is suitable for the ITER application. Therefore a key design parameter is the cutoff frequency of the ridged waveguide.

2. T-shaped ridged waveguide with arms

In this paper, a T-shaped ridged waveguide with arms[2] is used to lower its cutoff frequency without using small gap. Figure 4 shows a T-shaped ridged waveguide with two arms on its both sides. The waveguide is a hollow conducting cylindrical tube with a cross section in the xy plane and is uniform along the z axis of the propagating direction. The waveguide is empty with the electrical parameters ε, μ. The waveguide walls are assumed to have infinite conductivity. According to these assumptions, electric and magnetic fields are expressed by the potential ϕ, and the functional $\Gamma(\phi)$ for FEM is given as follows.

$$\vec{E} = -j\omega\mu\vec{\nabla} \times \phi\vec{z} \tag{3}$$

$$\vec{H} = \vec{\nabla} \times \vec{\nabla} \times \phi\vec{z} \tag{4}$$

$$\Gamma(\phi) = \frac{1}{4}\mu k^2 \int\int (k^2\phi^2 - \phi_x^2 - \phi_y^2)dxdy \tag{5}$$

where the subscripts x and y denote the partial derivative of ϕ by x and by y. Figure 5 shows the magnitude of the electric field distribution along the ridge surface at cutoff frequency. The electric field is almost uniform from the waveguide center to the corner C_3, and decay abruptly beyond a corner C_4. The electric field profile is concentrated between the waveguide center and the corner C_4, which indicates that this waveguide is a folded T-shaped ridged waveguide. The cutoff frequency f_c is approximated by the following equation[3][4],

$$f_c = \frac{c}{\pi}\sqrt{\frac{P_1}{(W-2P_2+2P_3)WH}} \tag{6}$$

where c is the velocity of light. The errors of the approximation shown in Table 2 increase for long arms, however, an idea of the folded T-shaped ridge is useful to understand the waveguide cutoff frequency.

The waveguide impedance Z_r is a parameter for the transmission-line theory discussed in the next section. Since most of the energy is concentrated between the waveguide center and the corner C_4, the waveguide impedance $Z_{r\infty}$ at $k=\infty$ is given by the parallel-plate model whose width and gap spacing between plates are $W-2P_2+2P_3$ and P_1.

$$Z_{r\infty} = 120\pi\frac{P_1}{W-2P_2+2P_3} \tag{7}$$

Table 1 shows $Z_{r\infty}$ calculated by the FEM and by the parallel-plate model, in which we obtain fine agreement between them. Therefore, the waveguide impedance of the T-shaped ridged waveguide with arms is approximated by the following equation

$$Z_r = 120\pi\frac{k}{\sqrt{k_{cr}^2-k^2}}\frac{P_1}{W-2P_2+2P_3} \tag{8}$$

The FEM analysis gives the waveguide characteristics and electric field distribution in detail, however, the cutoff frequency and the waveguide impedance is obtained by the simple model discussed in the above.

3. Analysis of ceramics-free coaxial waveguide

This section presents the analysis of ceramics-free coaxial waveguide shown in Fig. 6. Its inner conductor is a concave shape to obtain good impedance matching at the posts. The cross section at the post can be seen as a T-shaped ridged waveguide with arms. Since propagating energy is concentrated in a region between the concave conductor and the waveguide inner wall, the post under the concave conductor does not disturb the fields in this waveguide.

Two sections of the waveguide, the TEM (Transverse Electromagnetic) waveguide and the ridged waveguide, are characterized by the waveguide impedance and the propagation wavenumber as the transmission-line theory. Figure 7 shows the transmission-line model of the ceramics-free waveguide. The inner conductor is supported by three posts and the waveguide is terminated at 0-0' to the antenna of its input impedance Z_A. We assume an optimized antenna parameter for the ITER plasma in the calculation of Z_A[5][6]. The notation i-i' (i<7) denotes the junction between the TEM and the ridged waveguide. The waveguide length for the ITER is around 10m, which enables the stub tuning at the waveguide feed point 7-7' outside the cryostat. Therefore, the feed point is assumed to be matched to the waveguide in the following analysis model. The wave impedance of the TEM section Z_t is equivalent to $Z_{r\infty}$, because identical concave conductor is used for the TEM section in the ceramics-free waveguide. The impedance at i-i' in Fig. 7 is calculated by following equations by transmission line theory[7].

$$Z_{2m-1(2m-1)'} = Z_t\frac{Z_{2m-2(2m-2)'}+jZ_t\tan(kL_{2m-1})}{Z_t+jZ_{2m-2(2m-2)'}\tan(kL_{2m-1})} \tag{9}$$

$$Z_{2m2m'} = Z_r\frac{Z_{2m-1(2m-1)'}+jZ_t\tanh(\gamma_r L_{2m})}{Z_r+jZ_{2m-1(2m-1)'}\tanh(\gamma_r L_{2m})} \tag{10}$$

To estimate the maximum radiated power from the antenna, we define a power handling capability P_h as the radiated power P_o normalized by square the maximum voltage V_{max} in the waveguide.

$$P_h = \frac{P_o}{V_{max}^2} = \frac{Real1\times\frac{1}{Z_{77'}}}{V_{max}^2} \tag{11}$$

If we know the maximum voltage V_b not to cause the breakdown in the waveguide, we obtain the maximum power handing capability by multiplying P_h by V_b^2. Figure 8 shows the power handling capability for the cutoff

frequency of the ridged waveguide 50, 60, 70, and 80MHz, where a 10m long inner conductor is supported by two 50cm ridged waveguide sections. When the maximum voltage in the waveguide is 50kV (the magnitude of the electric field strength 20kv/cm for the minimum gap spacing 2.5cm), 3MW power handling capability is obtained for P_A=0.0012 in Fig. 8. The P_A is less than 0.0012 below 17MHz and for 45~55MHz when the cutoff frequency is higher than 70MHz. The cutoff frequency should be lower than 50MHz to obtain $P_A \geq 0.001$ within the frequency range of ITER IC system 15~80MHz.

4. Experiments

This section will verify the transmission-line theory by several one-tenth scale models. To measure resonant frequencies, we terminated a short or an open circuit to the model waveguide instead of an antenna. Though electrical short is given by attaching a conducting plate at the waveguide end, an ideal open circuit can not be obtained. We terminated no load to the waveguide, because the model waveguide impedance is 5~20Ω which is much smaller than the wave impedance in free space and gives an open condition approximately. The input impedance at the feed point for these loads become zero or infinite for at the resonance, and we obtain calculated resonant frequencies.

Three one-tenth scale models were used in the experiments. They are made by aluminum, and its parameters are shown in Table 1. A model 1 is a TEM waveguide with no ridged waveguide support, and an inner conductor is supported by dielectric posts. Models 2 and 3 are the ceramics-free waveguides with two/three ridged waveguide supports. The cutoff frequencies of the ridged waveguide section are 503.90MHz for model 2 and 447.95MHz for model 3 calculated by the FEM. Table 3 shows measured and calculated resonant frequencies. Measured results agree with calculated ones within 10% errors, which indicates the validity of the transmission-line theory. It is important to verify our theory terminating the scale model with an impedance which simulates a plasma load. However it is not easy to obtain the load which simulates the same frequency characteristics with a plasma. It will be left for the future problem.

5. Conclusion

We have proposed the ceramics-free coaxial waveguide for ITER IC (15~80MHz) system in which the TEM waveguide is supported mechanically by T-shaped ridged waveguide. The concept of this waveguide is applied to the mechanical support of the inner conductor of the coaxial-line. The power handling capability more than 3MW is evaluated by using the transmission-line theory and the optimized antenna impedance considering the ITER plasma parameters. We verified the theory experimentally by one-tenth scale models. The power handling capability of the ceramics-free waveguide depends on the impedance matching between the waveguide and the antenna input impedance, when the ridged waveguide section is much shorter than the wavelength and has low cutoff frequency. In addition, the cutoff frequency should avoid the vicinity of the frequency for the heating and the current drive. These conditions give various combination of TEM waveguide and the mechanical support section other than the example of this paper.

References

1. V.Parail et al , ITER Documentation Series, No. 32, IAEA, Vienna, 1991.
2. H.Kimura et al., Japan Atomic Energy Research Institute Report JAERI-M 91-094, 1991.
3. F.W.Perkins, Bull. Amer. Phys. Soc., vol. 26, p. 929, Sept. 1981.
4. H.Arai and N.Goto, IEEE Trans. Plasma Sci., vol. ps-13, no. 6, pp. 582-686, Dec. 1985.
5. H.Kimura et al., Proc. 4th Int. Symp. Rome, 1984 ,vol. 2, pp.1128-1135.
6. D.E.Post et al., ITER Documentation Series, No. 21, IAEA, Vienna, 1991.
7. R.E.Collin, "Field theory of guided waves," IEEE Press, New York, 1991.
9. H.Arai et al., IEEE Trans. Plasma Sci., vol. 21, no.3. pp.265-270, Jun. 1993

This work was supported by Japan Atomic Energy Research Institute.

Talbe 1 Reflection coefficient at junction
fc is center frequency for stub

f/fc	Γ	Γ^2
0.5(1.5)	0.447	0.2
0.6(1.4)	0.341	0.116
0.7(1.3)	0.246	0.060
0.8(1.2)	0.160	0.025
0.9(1.1)	0.078	0.006
1.0	0.0	0.0

Talbe 2 Cutoff frequency and waveguide impedance
FEM is Finite Element Method, FTR is Folded T-shaped Ridge model,
PPW is Parallel Plate Waveguide model,
W=300, H=700, $T_1=T_2=T_3=35$, $P_1=P_2=25$ (mm), $k_1=K_2=0$

P_3(mm)	f_c(MHz)		$Z_{TE\infty}(\Omega)$	
	FEM	FTR	FEM	PPW
100	49.21	49.12	17.12	20.94
300	40.94	35.73	10.65	11.10
500	36.39	29.40	7.55	7.54

Talbe 3 Resonant frequency (MHz) of one-tenth model waveguide
W=35, H=75, $T_1=12$, $T_2=T_3=2.4$(mm), $k_1=k_2=0$.
Model 1 is TEM waveguide without ridged waveguides,
Parameters of Model 2 are $L_1=L_5=158.7$, $L_3=158.6$, $L_2=L_4=12.0$,
$P_1=6$, $P_2=2.5$, $P_3=27.6$(mm),
Parameters of Model 3 are $L_1=L_3=L_5=L_7=116.0$, $L_2=L_4=L_5=12.0$,
$P_1=4.2$, $P_2=2.5$, $P_3=27.6$(mm).

model 1		model 2		model 3	
theory	measured	theory	measured	theory	measured
150.0	139.9	185.0	201.4	187.4	195.8
300.0	294.7	328.2	312.2	334.2	339.7
450.0	413.5	463.2	446.5	456.0	416.7
600.0	593.0	615.1	599.0	596.8	610.1

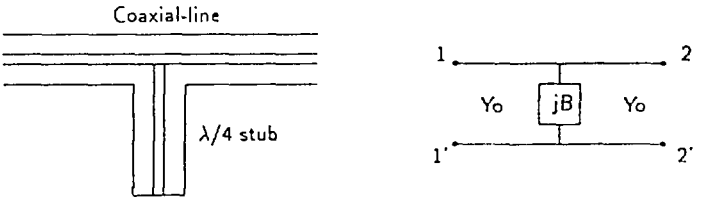

Figure 1: Equivalent circuit for junction

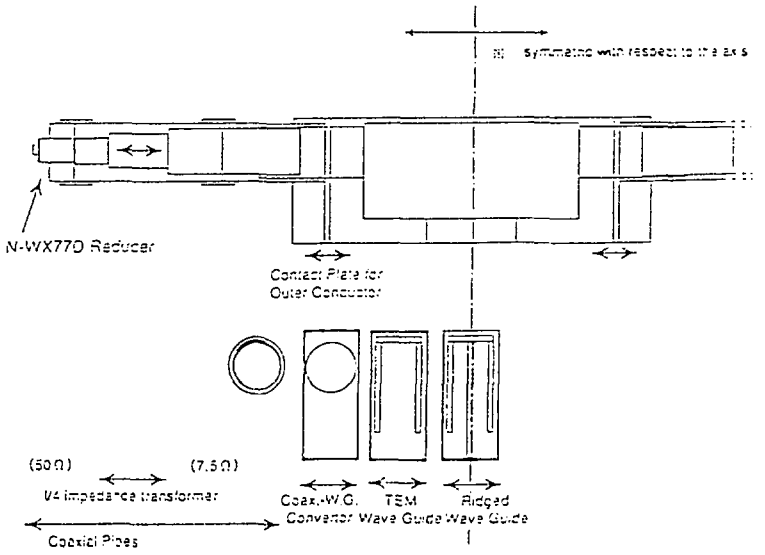

Figure 2: Ceramics-free coaxial waveguide

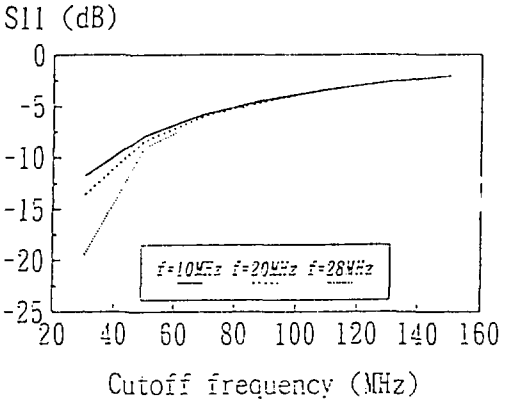

Figure 3: Reflection from ridged waveguide of l=50cm

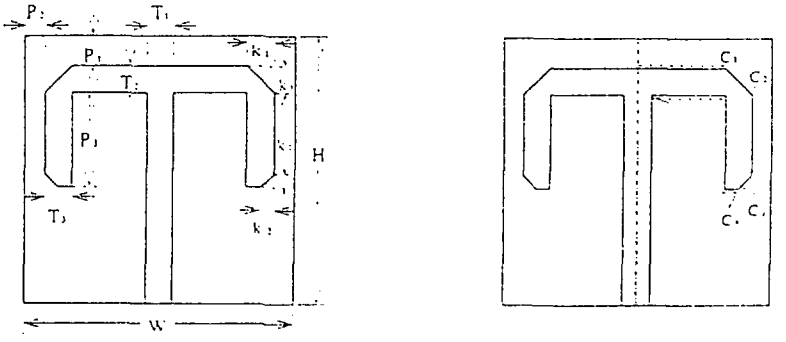

Figure 4: Cross section of T-shaped ridged waveguide with arms

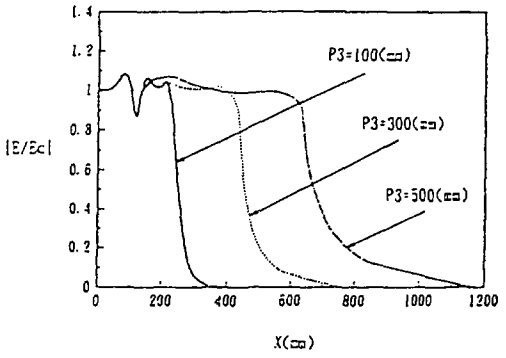

Figure 5: Electric field distribution along ridge
$T_1=T_2=T_3=30$, $P_1=P_2=25$, $k_1=25$, $k_2=12.5$, w=300, H=700(mm).

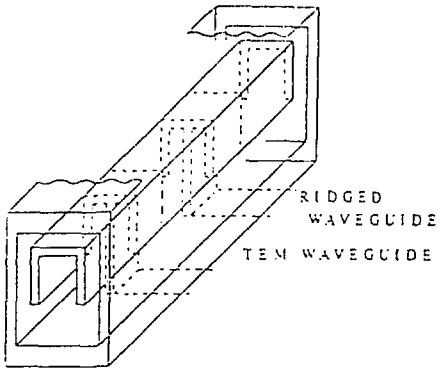

Figure 6: Ceramics-free coaxial waveguide

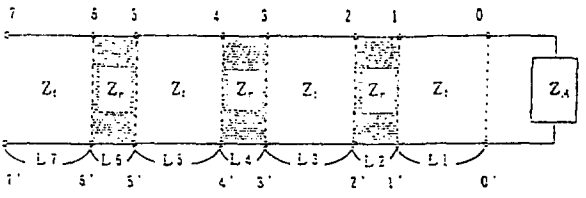

Figure 7: Transmission line model of ceramics-free

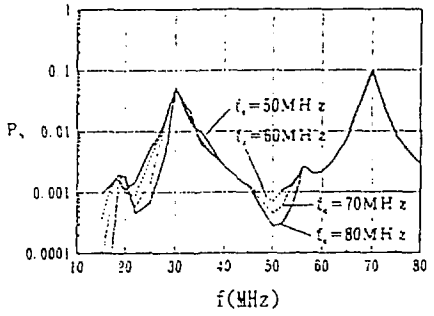

Figure 8: Normalized radiation power as a function of frequency
$Z_t=7.5\Omega$, $L_2=L_4=50$cm